Noname manuscript No.
(will be inserted by the editor)

Allee effects introduced by density dependent phenology

Timothy J. Pervenecki · Sharon Bewick · Garrett Otto · William F. Fagan · Bingtuan Li

Funding: Timothy J Pervenecki was partially supported by the National Science Foundation under Grant DMS-1225693; Sharon Bewick was partially supported by the National Science Foundation under Grant DMS-1225917; Garrett Otto did not receive funding to assist in the preparation of this manuscript; William F. Fagan was partially supported by the National Science Foundation under Grants DMS-1225917 and NNA-2127271; Bingtuan Li was partially supported by the National Science Foundation under Grants DMS-1225693, DMS-1515875, and DMS-1951482.

Declarations of interest: none

Timothy J. Pervenecki
Department of Mathematics and Computer Science, University of Wisconsin-Superior, Superior, WI 54880

Sharon Bewick
Department of Biological Sciences, Clemson University, Clemson, SC 29631

Garrett Otto
Department of Mathematics, SUNY Cortland, Cortland, NY 13045

William F. Fagan
Department of Biology, University of Maryland, College Park, MD 20742

Bingtuan Li (corresponding author)
bing.li@louisville.edu
Department of Mathematics, University of Louisville, Louisville, KY 40059

Allee effects introduced by density dependent phenology

Abstract We consider a hybrid model of an annual species with the timing of a stage transition governed by density dependent phenology. We show that the model can produce a strong Allee effect as well as overcompensation. The density dependent probability distribution that describes how population emergence is spread over time plays an important role in determining population dynamics. Our extensive numerical simulations with a density dependent gamma distribution indicate very rich population dynamics, from stable/unstable equilibria, limit cycles, to chaos.

Keywords Phenology · Allee Effect · Overcompensation

1 Introduction

Phenology, or seasonal biological timing, is an issue of widespread interest in ecology. Biologists studying phenology seek to understand how temporal variation in a particular transient process (e.g., a pulse of births, or a transition between life stages), matters to the dynamics of the larger system (Miller-Rushing et al. 2010; Lynch et al. 2014; Bewick et al. 2016; Encinas-Viso et al. 2012; Chmura et al. 2019). In ecological systems, changes in phenology can involve changes in the start time of a process within a season and/or changes in the temporal distribution (i.e., the synchrony) of that process (CaraDonna et al. 2014; Calabrese and Fagan 2004; Chmura et al. 2019).

As but one example, phenology plays a particularly important role in the dynamics of invasive plants and animals, which is an area of huge interest in applied ecology (Keller and Shea 2021). For instance, in-depth investigations have explored the linkage between phenological asynchrony and invasion success for a variety of forest species (e.g., Logan and Powell 2001; Ward and Masters 2007; Robinet et al. 2008). For example, in the case of the invasion of non-native gypsy moth (*Lymantria dispar*), asynchrony among breeding adults arises from a variety of biological mechanisms, such as variation in development rates among juvenile insects (Robinet et al. 2007, 2008; Gascoigne et al. 2009). This reproductive asynchrony creates opportunities for some females to go mateless, and this reduced level of reproduction slows the rate of spatial spread of the population (Johnson et al. 2006; Tobin et al. 2007). In some cases, such variation in developmental rates may be genetically driven (Gray 2004). Alternatively, phenological variation may arise through small-scale differences in environmental conditions (e.g., temperature, elevation, or other

microclimatic features; Walter et al. 2015), which cause individuals to develop at different rates, even over distances linked by dispersal.

In the past, it has been convenient to model phenology using time-dependent functions (i.e., creating non-autonomous equations) because this created a tight conceptual linkage to the kinds of empirical data that motivated the research (Calabrese et al. 2008; Fagan et al. 2010). For example, ecologists routinely record the onset and duration of particular life stages (e.g., adult butterflies and flowering plants), and such data lend themselves to being summarized as a function of time (e.g., as a beta or gamma distribution). However, phenology may be a more complicated process than that suggested by a simple time-dependent function. Indeed, a variety of studies, particularly in flowering plants, suggest a role for density to shape phenology within a population (Thomas and Bazzaz 1993; Donohue et al. 2000; Weinig et al. 2006; Vermeulen 2015). Both advances and delays in phenological distributions relative to seasonal benchmarks may be driven by density. For example, for several plants such as *Phaseolus Vulgaris L.* (Abubaker 2008) and the cleistogamous (closed, usually self-pollinating) flowers of *Impatiens capensis* (Schmitt et al. 1987), low densities can delay flowering seasonally whereas high densities can advance flowering. In (Schmitt et al. 1987) they hypothesize that this could be due to a stress related threshold needed to trigger flowering. Plant density has an opposite effect on the chasmogamous (open, usually cross-pollinating) flowers of *Impatiens capensis* (Schmitt et al. 1987), with higher densities causing later flowering. Because population density can affect phenology, in this paper we switch from modeling phenology as a purely time-dependent process to modeling phenology as both time- and density-dependent. This switch to a model in which phenology depends on density is advantageous because it allows us to explore the mechanistic foundation of phenology-induced Allee effects in more detail. Previous work (e.g., Calabrese et al. 2008; Rhainds and Fagan 2010; Lynch et al. 2014) all discussed phenology-dependent Allee effects as the indirect consequence of male and female reproductive activity being misaligned in time. Here, we forego a two-sex modeling approach in favor of one that in which the effect of density is directly modeled.

A *demographic Allee effect* is a positive relationship between the overall individual fitness (often quantified by the per capita population growth rate) and population size or density (Courchamp et al. 2008). A demographic Allee effect can be subdivided into two categories, a strong Allee effect and a weak Allee effect, with the difference being that in the case of a strong Allee effect there exists a density threshold that must be overcome for the population to persist.

Several well known mechanisms for the Allee effect exist, including mate limitation (e.g., Berec et al. 2007; Davis et al. 2004), cooperative defense (e.g., Courchamp et al. 2008; Mooring et al. 2004; Clutton-Brock et al. 1999), cooperative feeding (e.g., Berec et al. 2007), and environmental conditioning (e.g.,

Rinella et al. 2012; Kramer et al. 2009). Here, we explore a different, arguably new, mechanism for generating the Allee effect: density dependent phenology. Several biological scenarios would fit within this framework. For example, crowding experienced by adults could induce different levels of so-called 'maternal effects' (Roach and Wulff 1987) in their offspring (e.g., higher density adults may have offspring that grow more slowly because crowded adults have fewer resources to allocate to each of their offspring). One of the most widely known mathematical treatments of maternal effects are those of Turchin (1990), in which maternal crowding introduces a form of lagged density dependence in population timeseries of forest insects. If maternal effects influence offspring growth rates rather than simply mortality rates, it creates a potential linkage between growing conditions in one generation and phenology in the next generation as has been shown for winter moths *Operophtera brumata* (Van Asch et al. 2010). Such effects are similar to so-called scramble competition in population ecology (Nicholson 1954) except that the focus is not on survivorship as the metric of success but rather development rate. Understanding of maternal effects is also well developed in some plant species (Galloway 2002; Donohue 2009; Galloway and Burgess 2009) wherein the growing conditions of adult plants carry over to affect several measures of performance in the next generation, including the phenology of seed germination.

2 The Model

We study a hybrid dynamical model (Eskola and Geritz 2007; Eskola and Parvinen 2010; Mailleret and Lemesle 2009; Lewis and Li 2012; Otto et al. 2018) that models the population dynamics of an annual species. As outlined above, relevant species include both annual plants and insects, but we will relate the model to an annual plant system and use relevant biological language. We use an ordinary differential equation to consider within-season phenology as a continuous process and couple that with a difference equation that governs the transition between years. In keeping with our framework of density-mediated maternal effects, we focus on the process of seed production, examining how maternal density shapes the phenology of that process. We do not explicitly model change in size of seeds, only their population density.

We assume that seed production takes place for $0 < t \leq 1$ each year. In year n, A_n denotes the density of reproductive adult plants at time $t = 0$, and $J(A_n, t)$ denotes the seed population density in the reproduction season $0 < t \leq 1$. We assume that each adult produces an average of α seeds. We use $g(A_n, t)$ to represent the density-dependent probability density function, where the fraction of the adult population which produce their seeds at time t is given by $g(A_n, t)$. The density of seeds at $t = 0$ is 0 and we assume the adults experience a death rate of μ for $0 < t \leq 1$. The rate of seed production at time t

in the nth season is thus given by $\alpha e^{-\mu t} A_n g(A_n, t)$. This can be explained by noting that without adult plant death, $\alpha A_n g(A_n, t)$ would be the number of seeds produced at time t, however by time t only $e^{-\mu t}$ of the adults that would produce seeds at time t are still viable. Natural death for seeds is linear with the coefficient ν and additional seeds mortality mediated through seed crowding (Janzen 1970; Connell 1971) which is quadratic with the coefficient β according to the law of mass action (see, e.g., Thieme 2003). At the end of the reproductive season ($t = 1$), all the adults die, and the population of the following season is recruited from the seeds that survive the winter. We use γ to denote the product of the winter survival rate of the seeds, the conversion rate of the juveniles from the seeds, and the survival rate of the juveniles plants converting to the adults. Adults and seeds from the previous season are assumed to not carry over to the next season. The population dynamics are governed by

$$\begin{aligned} J_t &= \alpha A_n e^{-\mu t} g(A_n, t) - \nu J - \beta J^2, \\ J(A_n, 0) &= 0, \\ A_{n+1} &= \gamma J(A_n, 1). \end{aligned} \tag{1}$$

The probability distribution g reflects intra-year seasonal variation in phenology; that is, the function captures when reproduction (or more generally, a demographic process) starts and how asynchronous life stages are within a reproduction season. The phenology function g depends on the adult population in the previous year. This is consistent with the idea that density-dependent phenology can arise through maternal effects, as was discussed in the Introduction. Specifically, we envision scenarios in which the local crowding conditions experienced by adult plants influence their growth rate and thus the time in the season at which they produce mature seeds. In general $g(A, t)$ is defined for $0 \leq t < \infty$. If the upper bound of the support of $g(A, t)$ is bigger than 1, some organisms cannot reproduce. This leads to the case where changes in phenology due to climate change lead to a localized species becoming invasive or an invading species becoming extinct.

Our goal is to show that model (1) can produce a strong Allee effect as well as overcompensation. Analytical results regarding the presence of an Allee effect are given in the next section. In Section 3, numerical simulations are provided to demonstrate the existence of Allee effect and overcompensation with a density dependent gamma distribution. Section 4 includes some concluding remarks and discussions.

3 Analytical results

In this section we present analytical results regarding the existence of an Allee effect in model (1). We begin with the following hypothesis.

Hypothesis 1 *For $A \geq 0$ and $0 \leq t \leq 1$, $g(A,t)$ is nonnegative and bounded, $\int_0^\infty g(A,t)dt = 1$, and $g(A,t)$ has continuous partial derivatives with respect to A and t up through order 2.*

This hypothesis indicates that $g(A,t)$ is a smooth density dependent probability distribution of time.

Under Hypothesis 1, model (1) is well-posed. The right-hand side of the differential equation in (1) is locally Lipschitzian in J as $-\nu J - \beta J^2$ is continuously differentiable in J. Theorem 3.1 - Theorem 3.3 and Exercise 3.4 in Chapter 1 of Hale (1980) show that the initial value problem

$$J_t = \alpha e^{-\mu t} g(A,t)A - \nu J - \beta J^2, \ J(A,0) = 0,$$

has a unique solution $J(A,t)$, with the property that $\frac{\partial^2}{\partial A^2}J(A,t)$ is continuous for $0 \leq t \leq 1$ and $A \geq 0$. Let

$$f(A) = \gamma J(A,1).$$

Clearly $f(0) = 0$.

We summarize these results in the following proposition.

PROPOSITION 1 *Assume that Hypothesis 1 holds. Then $A_{n+1} = f(A_n)$ in (1) where $f''(A)$ is continuous for $A \geq 0$ and $f(0) = 0$.*

In general the differential equation in (1) cannot be analytically solved, and consequently the function f cannot be explicitly given. We are, however, able to use the connection between f and $g(A,t)$ to establish explicit conditions for the presence of an Allee effect and to determine when the Allee effect is strong. An Allee effect arises when the per-capita offspring number increases with population density over some range for small populations, i.e., $\frac{f(A)}{A}$ increases for small positive A. Note

$$\left(\frac{f(A)}{A}\right)' = \frac{f'(A)A - f(A)}{A^2}, \quad (f'(A)A - f(A))' = f''(A)A, \quad (f'(A)A - f(A))|_{A=0} = 0.$$

This and continuity of $f''(A)$ show that for small positive A, the sign of $(\frac{f(A)}{A})'$ is same as that of $f''(0)$, if $f''(0) \neq 0$. Therefore for small positive A, $\frac{f(A)}{A}$ increases if $f''(0) > 0$ and $\frac{f(A)}{A}$ decreases if $f''(0) < 0$. On the other hand, 0 is asymptotically stable for f if $|f'(0)| < 1$.

The following lemma provides explicit formulas for both $f'(0)$ and $f''(0)$.

Lemma 1 *Assume that Hypothesis 1 holds. Then*

$$f'(0) = \alpha\gamma \int_0^1 g(0,t)e^{-\mu t-(1-t)\nu}dt, \ \textit{and}$$

$$f''(0) = 2\alpha\gamma \int_0^1 \left(\left[\frac{\partial}{\partial A} g(A,t) \right] \Big|_{A=0} \right) e^{-\mu t-(1-t)\nu}dt$$
$$- 2\alpha^2\beta\gamma \int_0^1 g(0,t)e^{-\mu t-(1-t)\nu} \int_t^1 e^{-\nu s} \int_0^s g(0,r)e^{-\mu r}e^{\nu r}drdsdt.$$

The proof for this lemma is provided in the Appendix.

This lemma shows $f'(0) \geq 0$. We therefore have that 0 is asymptotically stable if $f'(0) < 1$. Recall $f''(0) > 0$ indicates the presence of an Allee effect. These and Lemma 1 lead to the following theorem.

Theorem 1 *Assume that Hypothesis 1 is satisfied. The following statements hold for model* (1)*:*
(i) The equilibrium 0 *is asymptotically stable if*

$$\alpha\gamma \int_0^1 g(0,t)e^{-\mu t-(1-t)\nu}dt < 1. \tag{2}$$

(ii) There exists an Allee effect if

$$\begin{aligned} &\int_0^1 \left(\left[\frac{\partial}{\partial A}(e^{-\mu t}g(A,t)) \right] \Big|_{A=0} \right) e^{-\mu t-(1-t)\nu}dt \\ &> \alpha\beta \int_0^1 e^{-\mu t}g(0,t)e^{-(1-t)\nu} \int_t^1 e^{-\nu s} \int_0^s e^{-\mu r}g(0,r)e^{\nu r}drdsdt. \end{aligned} \tag{3}$$

The condition in (i) indicates that the equilibrium 0 is asymptotically stable if for a given $g(A,t)$ one of α, γ is small or one of μ and ν is large, or if for relatively large α and γ relatively small μ and ν, the distribution of $g(A,t)$ at $A = 0$ is relatively low on $[0,1]$ in the sense of (2).

The condition in (ii) shows there exists an Allee effect if for appropriate parameter values the distribution of $\frac{\partial}{\partial A}(e^{-\mu t}g(A,t))$ at $A = 0$ is relatively high and the distribution of $g(A,t)$ at $A = 0$ is relatively low on $[0,1]$.

The inequality in (ii) is a sharp condition for the existence of Allee effect. It is equivalent to $f''(0) > 0$. If it is reversed, there is no Allee effect. In the case of that $g(A,t)$ is density-independent, i.e., $g(A,t) = g(t)$, the left hand side of the inequality is zero and hence this inequality is reversed, so that there is no Allee effect in (1).

Under conditions (2) and (3), in order for (1) to have a strong Allee effect, there must exist an Allee threshold, which is determined by the presence of a positive equilibrium. We develop necessary and sufficient conditions for the existence of a positive equilibrium. Let

$$B(A,t) = \gamma J(A,t)/A,$$

with $A > 0$. Under condition (2) (which implies $f(A) < A$ for small positive A), a sufficient and necessary condition for $f(A)$ to have a positive equilibrium is that there exists $A > 0$ such that $\gamma J(A,1) = f(A) > A$, or equivalently $B(A,1) > 1$. The initial value problem (1) with A_n replaced by A shows

$$B_t = \alpha\gamma e^{-\mu t} g(A,t) - \nu B - \frac{\beta}{\gamma} A B^2, \quad B(A,0) = 0, \tag{4}$$

or equivalently

$$(B(A,t)e^{\int_0^t (\nu + \frac{\beta}{\gamma} AB(A,s))ds})' = \alpha\gamma g(A,t) e^{-\mu t} e^{\int_0^t (\nu + \frac{\beta}{\gamma} AB(A,s))ds}, \quad B(A,0) = 0.$$

Integration shows that $B(A,t)$ satisfies the integral equation

$$B(A,t) = T[B](A,t) := \alpha\gamma \int_0^t g(A,\tau) e^{-\mu\tau - (t-\tau)\nu - \frac{\beta}{\gamma} A \int_\tau^t B(A,s)ds} d\tau. \tag{5}$$

This indicates that the solution $B(A,t)$ of (4) is a fixed point of the integral operator T. $T[B]$ is well defined for any nonnegative continuous function $B(A,t)$ for $t \in [0,1]$. An important property of T is

$$T[B](A,t) \le T[\tilde{B}](A,t), \quad \text{if } B(A,t) \ge \tilde{B}(A,t); \qquad T[B](A,t) \ge T[\tilde{B}](A,t), \quad \text{if } B(A,t) \le \tilde{B}(A,t). \tag{6}$$

This is due to the fact that the integrand in (5) decreases in B.

We construct a sequence of functions using T to approximate $B(A,t)$. Consider $B_n(A,t)$ given by

$$B_{n+1}(A,t) = T[B_n](A,t), \quad B_0(A,t) \equiv 0. \tag{7}$$

Here each $B_n(A,t)$ can be computed explicitly for a given n.

The following proposition shows that the sub-sequence $B_{2n}(A,t)$ increases to $B(A,t)$ and the sub-sequence $B_{2n+1}(A,t)$ decreases to $B(A,t)$.

PROPOSITION 2 *For $n = 0, 1, 2, ...$, $B_{2(n+1)}(A,t) \ge B_{2n}(A,t)$ and $B_{2(n+1)+1}(A,t) \le B_{2n+1}(A,t)$, and furthermore $\lim_{n\to\infty} B_{2n}(A,t) = \lim_{k\to\infty} B_{2n+1}(t) = B(A,t)$.*

The proof for Proposition 2 is provided in the Appendix.

We have the following theorem regarding the existence of a positive equilibrium and a strong Allee effect.

Theorem 2 *Assume that Hypothesis 1 holds. The following statements hold:*

i. There exists a positive equilibrium if there is $A > 0$ and $n_0 \ge 1$ such that $B_{2n_0}(A,1) > 1$.

ii. There exists no positive equilibrium if there is $n_0 \ge 0$ such that for all $A > 0$, $B_{2n_0+1}(A,1) < 1$.

iii. Assume in addition the conditions (2)-(3) hold. If there exists a positive equilibrium, then the smallest positive equilibrium represents the Allee threshold.

The proof for Theorem 2 is provided in the Appendix.

In general, it is difficult to find $B_n(A,t)$ when n is large. However it is easy to find $B_n(A,t)$ when n is small. Specifically using (7) we have

$$B_1(A,t) = \alpha\gamma \int_0^t g(A,\tau) e^{-\mu\tau-(t-\tau)\nu} d\tau, \quad B_2(A,t) = \alpha\gamma \int_0^t g(A,\tau) e^{-\mu\tau-(t-\tau)\nu-\frac{\beta}{\gamma}A\int_\tau^t B_1(A,s)ds} d\tau.$$

We have the following corollary of Theorem 2, which provides relatively simple sufficient conditions for the existence and nonexistence of a positive equilibrium.

Corollary 1 *Assume that Hypotheses 1 holds. The following statements hold:*

i. There exists a positive equilibrium if there is $A > 0$ such that

$$\alpha\gamma \int_0^1 g(A,\tau) e^{-\mu\tau-(1-\tau)\nu-\frac{\beta}{\gamma}A\int_\tau^1 B_1(A,s)ds} d\tau > 1.$$

ii. There exists no positive equilibrium if

$$\alpha\gamma \int_0^1 g(A,\tau) e^{-\mu\tau-(1-\tau)\nu} d\tau < 1$$

for all $A > 0$.

From this Corollary and Theorem 2 (iii), model (1) has a strong Allee effect if (2)-(3) and the condition in Corollary 1 (i) are satisfied.

The condition in (i) indicates that there there exists a positive equilibrium if for relatively large α and γ and relatively small μ, ν and β, the distribution of $g(A,t)$ for some $A > 0$ is large on $[0,1]$ in a certain sense.

The condition in (ii) shows that there is no positive equilibrium if for a given $g(A,t)$ one of α, γ is small or one of μ and ν is large, or if for relatively large α and γ relatively small μ and ν, the distribution of $g(A,t)$ for all A is relatively low on $[0,1]$ in a certain sense.

4 Numerical simulations

The MatLab code used in the simulations can be viewed at `https://github.com/glotto01/density-dependant-phenology`.

We use the gamma distribution to describe the density dependant phenology. Among the advantages of the gamma distribution are that it is continuous, has non-negative support, and the mean and variance can be independently controlled. Other advantages of gamma distributions without density dependence in the context of phenologically explicit models are discussed at length elsewhere (Calabrese et al. (2008)), and more applications of gamma distributions for phenology can be found in Bewick et al. (2016), Fagan et al. (2010), and Fagan et al. (2014). A density dependent gamma distribution takes the form of

$$g(A,t) = \frac{t^{k-1}\, e^{-\frac{t}{\theta}}}{\Gamma(k)\, \theta^k},$$

where the shape parameter k and scale parameter θ depend on A. The mean of the distribution is given by $\tau = k\,\theta$ and the variance is given by $\sigma^2 = k\,\theta^2$. It follows that $k = \frac{\tau^2}{\sigma^2}$ and $\theta = \frac{\sigma^2}{\tau}$. We will assume that the variance, σ^2 remains fixed regardless of the density, and that the mean time of production for seeds, τ, is given by a piecewise linear function, $\tau = \max(\sigma, aA + b)$. This linearity is motivated by Cao et al. (2016), where the mean day of flowering vs density is found to be roughly linear in the study of flowering phenology and sexual reproduction in the ephemeral herb *Cardamine hirsuta*. To insure our assumptions that $g(A,t)$ is continuous and bounded hold, it's necessary for $k \geq 1$, which in turn requires $\tau \geq \sigma$. It is also biologically reasonable to assume there is a lower limit on the mean production time of seeds.

Including this assumption we obtain

$$g(A,t) = \frac{t^{\left(\frac{\max(\sigma,aA+b)^2-\sigma^2}{\sigma^2}\right)}\, e^{-t\left(\frac{\sigma^2}{\max(\sigma,aA+b)}\right)}}{\Gamma\left(\frac{\max(\sigma,aA+b)^2}{\sigma^2}\right)\left(\frac{\sigma^2}{\max(\sigma,aA+b)}\right)^{\left(\frac{\max(\sigma,aA+b)^2}{\sigma^2}\right)}}\,.$$

We see that although the mean seed production time is linear in A, the phenology function g and model (1) are highly non-linear in A.

With these definitions of g, Theorem 1-(i) states that if

$$\alpha\gamma\, e^{-\nu}\left(1+\frac{\sigma^2(\mu-\nu)}{\max(\sigma,b)}\right)^{-\frac{\max(\sigma,b)^2}{\sigma^2}}\left(1-\frac{\Gamma\left(\frac{\max(\sigma,b)^2}{\sigma^2},\frac{\sigma^2}{\max(\sigma,b)}+\mu-\nu\right)}{\Gamma\left(\frac{\max(\sigma,b)^2}{\sigma^2}\right)}\right)<1$$

then the equilibrium 0 is asymptotically stable. Here $\Gamma(\cdot,\cdot)$ refers to the upper incomplete gamma function. The triple integral of part-(ii) of Theorem 1 does not admit a closed form solution for this definition of g. The integral in Corollary 1-(i) does not admit a closed form for this definition of g.

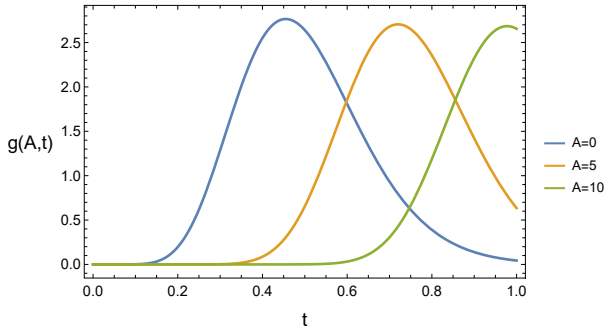

Fig. 1: The phenology distributions $g(A,t)$ for several population levels with $\sigma = 0.15,\ a = 0.05\ b = 0.5$.

Corollary 1-(ii) states that no positive equilibrium exists if

$$\alpha\gamma\, e^{-\nu}\left(1+\frac{\sigma^2(\mu-\nu)}{\max(\sigma,aA+b)}\right)^{-\frac{\max(\sigma,aA+b)^2}{\sigma^2}}\left(1-\frac{\Gamma\left(\frac{\max(\sigma,aA+b)^2}{\sigma^2},\frac{\sigma^2}{\max(\sigma,aA+b)}+\mu-\nu\right)}{\Gamma\left(\frac{\max(aA+\sigma,b)^2}{\sigma^2}\right)}\right)<1$$

for all $A > 0$. A closed form for the maximum value of the expression on the left hand side of the inequality does not appear to exist.

In Figure 1 we show how the phenology distribution varies with population when mean seeding time increases with density. In this figure the standard deviation is $\sigma = 0.15$ and the mean seeding time is $\tau = \max(0.15, 0.05A + 0.5) = 0.05A + 0.5$. We see that as the population increases the phenology distribution gets translated to the right, and for larger populations a significant portion fails to reproduce in the season.

In Figure 2 we show how the phenology distribution varies with population when mean seeding time decreases with density. In this figure the standard deviation is $\sigma = 0.15$ and the mean seeding time is $\tau = \max(0.15, -0.3A + 0.5)$. Note that τ will become fixed at 0.15 for $A > \frac{5}{3}$. We see that as the population increases the phenology distribution shifts to the left. Unlike Figure 1, we see that the skewness increases as the distribution shifts to the left due to the support being non-negative. We also note that for $A > \frac{5}{3}$, the distribution becomes an exponential distribution.

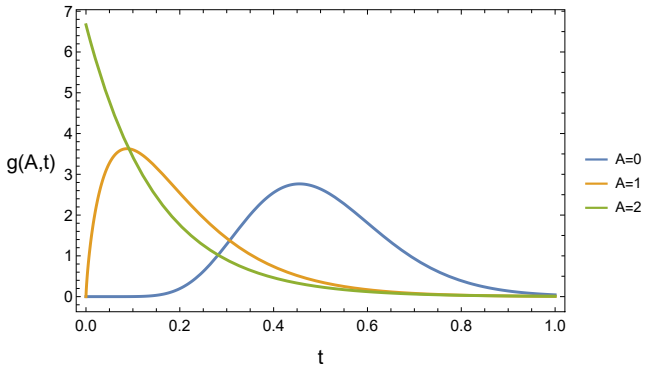

Fig. 2: The phenology distributions $g(A,t)$ for several population levels with $\sigma = 0.15,\ a = -0.3,\ b = 0.5$.

For results related to other distributions such as the uniform and generalized beta we refer the reader to the PhD thesis of Timothy Pervenecki (Pervenecki 2019).

It should be noted that by substituting $\tilde{J}(A,t) = \gamma J(A,t)$ into Model 1 we obtain

$$\tilde{J}_t = \gamma\alpha A_n e^{-\mu t} g(A_n,t) - \nu\tilde{J} - \frac{\beta}{\gamma}\tilde{J}^2,$$
$$\tilde{J}(A_n,0) = 0,$$
$$A_{n+1} = \tilde{J}(A_n,1).$$

Hence, without loss of generality, we may consider Model 1 with $\gamma = 1$.

4.1 Case 1: high seed mortality

In this simulation we assume the seed mortality rate is higher than that of the adults. The parameters used here are $\alpha = 10,\ \mu = 1,\ \nu = 5,\ \beta = 0.1,\ \sigma = 0.15,\ b = 0.5,\ \gamma = 1$. We use the parameter a as a bifurcation parameter to investigate how the density dependence of the mean seed production time effects the population dynamics. A positive a represents seed production being delayed with increased population density, whereas negative a represents seed production being advanced with increased density.

In Figure 3 we plot the growth function for several values of a. We see that a strong Allee effect and overcompensation occurs. The Allee effect can be understood in terms of higher populations delaying seed production, and thus exposing the seeds to less time at the higher mortality rate. The overcompensation can be understood by noting that large populations delay seed production to the point that much of the distribution falls outside of the season. This can be seen with $g(10,t)$ in Figure 1. It is worth noting the condition for the existence of a positive equilibrium given by the inequality in Corollary 1 is met for all

4 panels on Figure 3. For example, when $a = 0.05$ the integral on the lefthand side is greater than 1 for $3.02 < A < 11.01$ achieving a maximum of 1.57 at $A = 7.52$.

In Figure 4 we plot the equilibrium values of A. The blue curve is the stable extinction equilibrium, the red curve is the unstable Allee equilibrium. The black curve is the upper equilibrium which is stable where solid and unstable where dashed. Since the seeds face a rate of mortality five times higher than the adults, we would expect that delayed seed production would be favorable for the population so long as a significant fraction of the distribution falls within the $0 \leq t \leq 1$ season. In Figure 4 we see that there is no positive equilibrium until a is larger than roughly 0.01. At this point very large populations are able to delay seed production extensively enough that survival is possible. As a becomes larger, smaller populations are adequate to cause enough delay to stabilize the population. The Allee effect can be understood to take place due to higher densities being required to sufficiently delay seed production so that the high losses do not cause extinction.

In Figure 5, we see that the population dynamics undergo a period-doubling bifurcation to chaos as a increases. In Figure 6 we show a population time series for the growth functions in Figure 3- (b-d). The series are initiated with a population just slightly larger than the corresponding Allee threshold. Populations initiated below the Allee threshold will go extinct. The time series for Figure 3-(a) is not shown as it trivially leads to extinction. We see that for relatively small values of a we obtain a stable equilibrium, for intermediate values of a a period-4 solution emerges, and finally we see chaotic dynamics for large a.

It should be noted that as the seed mortality rate, ν, decreases from 5 while the other parameters are held fixed, the Allee effect disappears while a positive equilibrium remains. Theorem 1 (ii) allows us to determine the existence/non-existence of an Allee effect by examining the value of the integrals representing $f'(0)$ and $f''(0)$. For example with $\alpha = 10,\ \mu = 1,\ \beta = 0.1,\ \sigma = 0.15,\ b = 0.5,\ \gamma = 1,\ a = 0.5$, if we compute $f'(0)$ and $f''(0)$ using the formula in Lemma 1 with $\nu = 5$ we see that $f'(0) = 0.59$ and $f''(0) = 0.15$. $f'(0) < 1$ and $f''(0) > 0$ is indicative of a strong Allee effect. As ν decreases, $f'(0)$ increases and $f''(0)$ decreases. At $\nu = 3.76$, $f'(0) = 1$ and $f''(0) = 0.09$ indicating a transition to a weak Allee effect. As ν decreases to $\nu = 3.14$, $f'(0) = 1.32$ and $f''(0) = 0$ indicating the loss of the Allee effect. For $\nu < 3.14$, $f'(0) > 1$ and $f''(0) < 0$ indicating monotone dynamics.

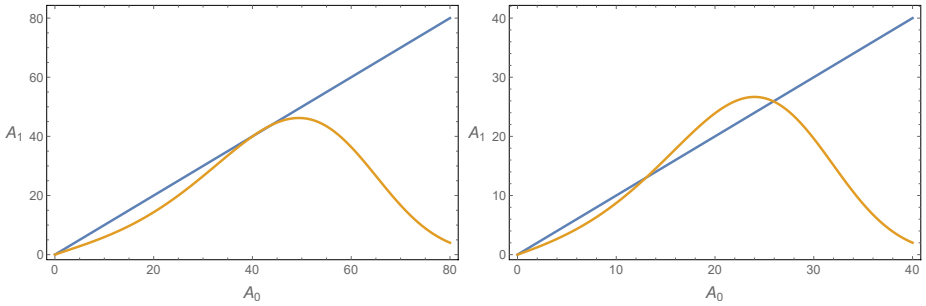

(a) $a = 0.01$

(b) $a = 0.02$

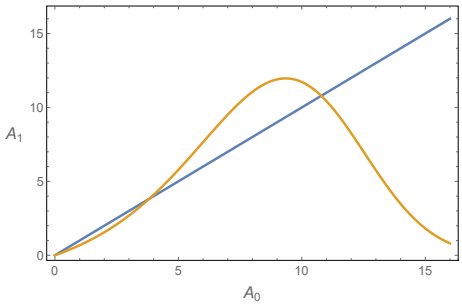

(c) $a = 0.05$

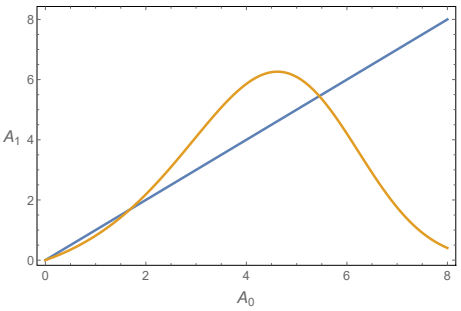

(d) $a = 0.1$

Fig. 3: The growth function for various values of a. We see as a increases the Allee threshold decreases, growth becomes stronger, and overcompensation also increases. Other parameters used are $\alpha = 10,\ \mu = 1,\ \nu = 5,\ \beta = 0.1,\ \sigma = 0.15,\ b = 0.5,\ \gamma = 1$.

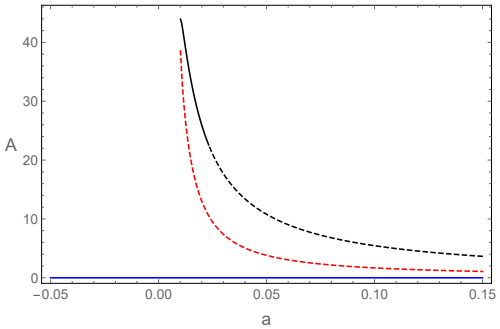

Fig. 4: The existence and stability of The equilibrium of Model 1 as a function of a. The other parameters used are $\alpha = 10,\ \mu = 1,\ \nu = 5,\ \beta = 0.1,\ \sigma = 0.15,\ b = 0.5,\ \gamma = 1$. The black curve is the carrying capacity, red is the Allee threshold, and blue is the extinction equilibrium. A solid curve indicates a stable equilibrium whereas dashed indicates unstable.

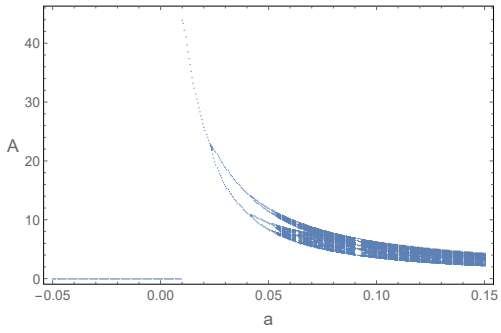

Fig. 5: A bifurcation diagram of the solutions as a function of a. We see period doubling cascade leading to chaos occurs as a increases. Other parameters used are $\alpha = 10,\ \mu = 1,\ \nu = 5,\ \beta = 0.1,\ \sigma = 0.15,\ b = 0.5,\ \gamma = 1$.

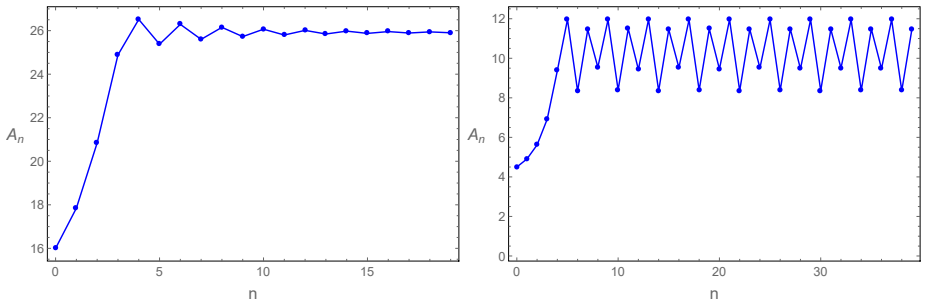

(a) $a = 0.02,\ A_0 = 16$ (b) $a = 0.05,\ A_0 = 4.5$

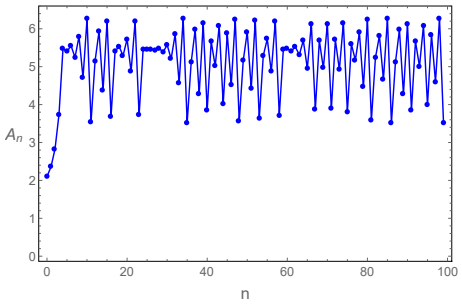

(c) $a = 0.1,\ A_0 - 0.8$

Fig. 6: A population time series corresponding to the growth functions in Figure 3-(b-d). The series are initiated with a population just slightly larger than the corresponding Allee threshold. We see an asymptotically stable equilibrium in (a), a period-4 solution in (b) , and chaotic dynamics in (c).

4.2 Case 2: high adult mortality

In this simulation we assume the seed mortality rate is lower than that of the adults. The parameters used here are $\alpha = 10,\ \mu = 5,\ \nu = 1,\ \beta = 0.1,\ \sigma = 0.15,\ b = 0.5,\ \gamma = 1$.

In Figure 7 we plot the growth function for several values of a. We note the growth function is monotone and has a strong Allee effect. The lack of overcompensation is due to the fact that τ has a lower bound of σ and thus seed production occurs within the season no matter how large the population is. This is in contrast to the high juvenile mortality case where with positive a, large populations push the seed production window outside of the season. For values of a producing a positive equilibrium (see Figure 8) the population dynamics will be simple, with populations initially above the Allee threshold converging to the stable upper positive equilibrium, and populations initially below the Allee threshold going extinct. This is illustrated in Figure 9, where we see the population monotonically increase from slightly above the Allee threshold towards the upper equilibrium. We see the growth function can have a discontinuity in its derivative, for example in panel (c) near $A_0 = 1.2$. This arises from the discontinuity of the derivative of $\tau = \max(\sigma, aA + b)$ when $\sigma = aA + b$.

In Figure 8, the blue curve is the stable extinction equilibrium, the red curve is the unstable Allee equilibrium, and the black curve is the upper stable equilibrium. We see the positive equilibrium does not form until a is less than about -0.1, and the Allee threshold continues to decrease as a decreases. As the adult stage has the high mortality rate in this case, we would expect advancing the seed production time would improve survival. In the formula for the mean seed production time, $\tau = \max(\sigma, aA + b)$, we see if aA is sufficiently negative there is a possibility of advancing the seed production time to a threshold where the species can survive. This explains the emergence of an Allee effect and why the Allee threshold decreases as a decreases. We also see the positive equilibrium saturates at a value near 4. This can be explained by noting if $aA + b < \sigma$ then $\tau = \sigma$ and the phenology, in effect, becomes fixed for sufficiently negative aA.

Similar to in Case 1, when the adult mortality rate, μ, decreases from 5 while the other parameters are held fixed, the Allee effect disappears while a positive equilibrium remains. For example with $\alpha = 10,\ \nu = 1,\ \beta = 0.1,\ \sigma = 0.15,\ b = 0.5,\ \gamma = 1,\ a = -0.3$, if we compute $f'(0)$ and $f''(0)$ using the formula in Lemma 1 we see that with $\mu = 5$, $f'(0) = 0.59$ and $f''(0) = 1.37$. $f'(0) < 1$ and $f''(0) > 0$ is indicative of a strong Allee effect. As μ decreases, $f'(0)$ increases and $f''(0)$ initially increases. At $\mu = 3.78$, $f'(0) = 1$ and $f''(0) = 1.54$ indicating a transition to a weak Allee effect. As μ decreases further eventually $f''(0)$ begins to decrease. At $\mu = 1.51$, $f'(0) = 2.85$ and $f''(0) = 0$ indicating the loss of the Allee effect. For $\mu < 1.51$, $f'(0) > 1$ and $f''(0) < 0$ indicating monotone dynamics.

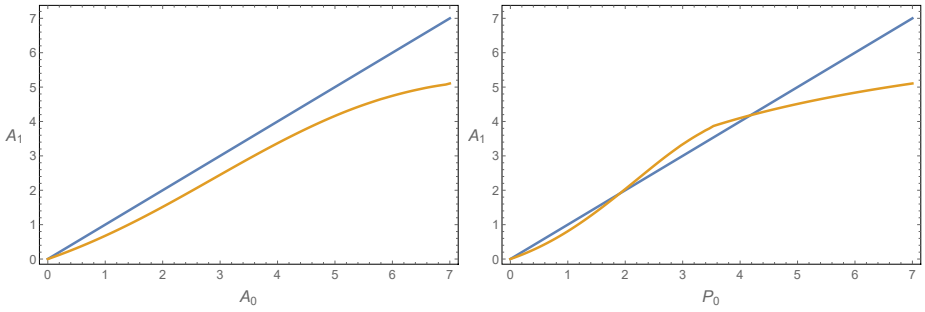

(a) $a = -0.05$ (b) $a = -0.1$

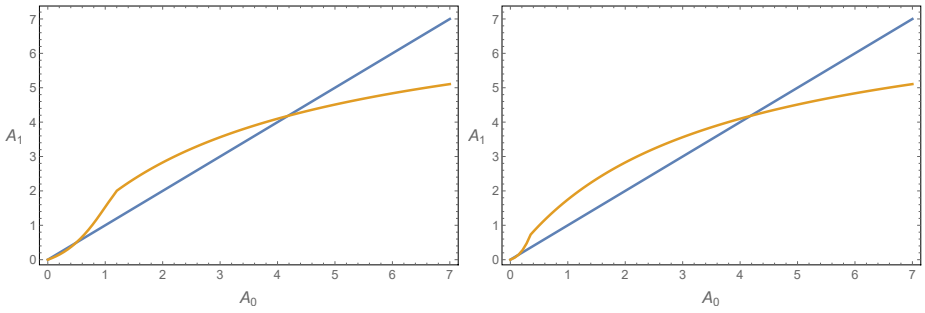

(c) $a = -0.3$ (d) $a = -1$

Fig. 7: The growth function for various values of a. We see that the Allee threshold decreases and growth becomes stronger as a becomes more negative. Other parameters used are $\alpha = 10,\ \mu = 5,\ \nu = 1,\ \beta = 0.1,\ \sigma = 0.15,\ b = 0.5,\ \gamma = 1$.

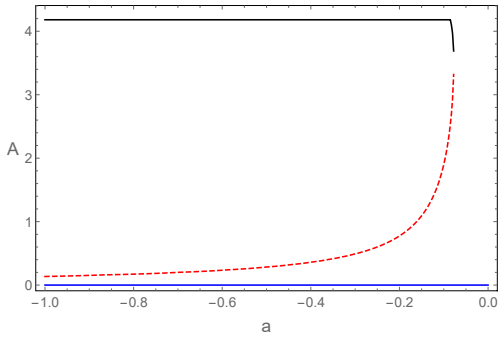

Fig. 8: The existence and stability of the equilibria of Model 1 as a function of a. The other parameters used are $\alpha = 10,\ \mu = 5,\ \nu = 1,\ \beta = 0.1,\ \sigma = 0.15,\ b = 0.5,\ \gamma = 1$. The black curve is the carrying capacity, red is the Allee threshold, and blue is the extinction equilibrium. A solid curve indicates a stable equilibrium whereas dashed indicates unstable. The carrying capacity saturates near $A = 4$ due to $aA + b < \sigma$, thus fixing τ to a value of σ.

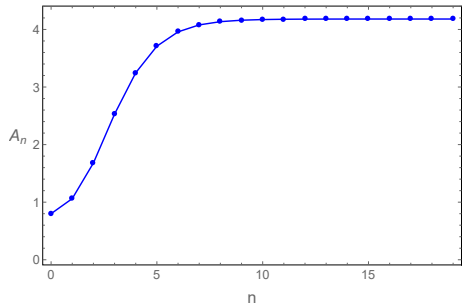

Fig. 9: A population time series corresponding to the growth functions in Figure 7-(c) with $a = -0.3$. We see the population asymptotically approaches the carrying capacity. The series was initiated with $A_0 = 0.8$

One aspect which we did not attempt to capture in this model are the effects of the interactions between the timing of seed production and the time available for seed development. We may imagine that the length of time for seed development might affect the seed quantity and quality. Including this may alter some of our conclusions.

5 Discussion

We developed a mathematical model of an annual species in which the timing of reproduction is governed by density. We obtained analytical integral conditions under which there is a strong Allee effect. Our results provide a new mechanism for generating Allee effects. Phenological differences (asynchrony) between males and females have been previously shown to generate Allee effects via the mate-limitation route in models that are explicitly two-sex (Calabrese and Fagan 2004; Calabrese et al. 2008). The result here is different because density is altering the phenological distribution of the population, creating the positive relationship between population growth rate and density that is necessary for a demographic Allee effect.

It is interesting to note that density dependent phenology can produce overcompensation as well. Our extensive numerical simulations with a density dependent gamma distribution indicate very rich population dynamics, from stable/unstable equilibria, limit cycles, to chaos. This richness of qualitative behavior is perhaps not surprising given the diverse scenarios in which overcompensation is known to drive complicated dynamics in population dynamics models. What is novel here is that the process that mediates the inter-year transitions in population density hinges on the way in which density controls the within-season timing of transition. Such seasonal timing is a variable of great interest in biology because it can be shaped by diverse factors including resource availability and climate change (e.g., Miller-Rushing et al. 2010; Vermeulen 2015).

The density dependent probability distribution $g(A,t)$ in model (1) describes how reproduction (or more generally, emergence into a population stage) is spread over time. This function plays an important role in generating Allee effects. When $g(A,t)$ is density independent, i.e., when $g(A,t)$ solely depends on time t, there is no Allee effect. The integral conditions (2) and (3) indicate that in order for the model to have an Allee effect, $\frac{\partial g(0,t)}{\partial A}$ should be relatively large and $g(0,t)$ should be relatively small for $t \in [0,1]$. This means biologically that at low population densities, the rate of change of $g(A,t)$ in A is large compared with $g(A,t)$ in $[0,1]$. According to Theorem 2 (i), there exists an Allee threshold if there is $A > 0$ such that $g(A,t)$ is relatively large for $t \in [0,1]$.

The framework developed in this paper can be also used to model phenology associated with maturation from seeds to reproductive adults influenced by density. Mechanistically, density may be linked to phenology via resource competition. For example, for some plants, density dependent phenology may emerge mechanistically because the degree of shading experienced by an individual may hinge on when in the growing season it emerges relative to other members of the population. That is, earlier plants emerging at low density may experience less shading than plants that emerge later in the season after other plants are already established (Callahan and Pigliucci 2002). Similar competitive processes may link density to flowering phenology as density-dependent resource acquisition during the vegetative stage may affect the transition from vegetative to reproductive growth, thereby determining bloom time (Schmitt et al. 1987; Abubaker 2008; Vermeulen 2015). Because of such links among density, access to resources, and relative success, phenology may be under selection in a density-dependent context (Callahan and Pigliucci 2002; Vincent and Brown 1984), and depending on the conditions, increased density may favor either early or late phenology (Vermeulen 2015).

Looking forward, the model could be further developed into a spatial model by adding a diffusion term. The interaction between the timing of juvenile emergence and the time available for juveniles to develop into adults is also worthy of investigation. Another possible extension would be to create a competition model, where one or both of the species has density dependent phenology. Modeling within such a competition framework could be especially interesting because it would allow for investigations of the evolution of phenology via an adaptive dynamics framework. Such studies would provide additional connections with relevant biology in that maternal effects have already been considered from an adaptive perspective (Galloway 2005; Van Asch et al. 2010) and because intriguing complex dynamics are possible when topics such as phenology (Eskola 2009) and resource allocation (Akhmetzhanov et al. 2011) are studied in an adaptive context.

6 Appendix

6.1 Proof of Lemma 1

Proof We derive explicit formulas for $f''(0)$ and $f'(0)$. The initial value problem of (1) is equivalent to

$$(J(A_n,t)e^{\int_0^t(\nu+\beta J(A_n,s))ds})' = \alpha g(A_n,t)e^{-\mu t}e^{\int_0^t(\nu+\beta J(A_n,s))ds}, \quad J(A_n,0)=0.$$

Integration shows

$$J(A_n,t) = \alpha A_n e^{-\int_0^t(\nu+\beta J(A_n,s))ds}\int_0^t g(A_n,\tau)e^{-\mu\tau}e^{\int_0^\tau(\nu+\beta J(A_n,s))ds}d\tau.$$

This gives an implicit year-to-year mapping

$$\begin{aligned} A_{n+1} &= f(A_n) := \gamma J(A_n,1) \\ &= \alpha\gamma A_n e^{-\int_0^1(\nu+\beta J(A_n,s))ds}\int_0^1 g(A_n,t)e^{-\mu t}e^{\int_0^t(\nu+\beta J(A_n,s))ds}dt \\ &= \alpha\gamma A_n \int_0^1 g(A_n,t)e^{-\mu t}e^{-\int_t^1(\nu+\beta J(A_n,s))ds}dt. \end{aligned} \tag{8}$$

Taking the first derivative yields

$$\begin{aligned} f'(A) = {} & \alpha\gamma\int_0^1 g(A,t)e^{-\mu t}e^{-\int_t^1(\nu+\beta J(A,s))ds}dt + \alpha\gamma A\int_0^1\left[\frac{\partial}{\partial A}g(A,t)\right]e^{-\mu t}e^{-\int_t^1(\nu+\beta J(A,s))ds}dt \\ & - \alpha\beta\gamma A\int_0^1 g(A,t)e^{-\mu t}e^{-\int_t^1(\nu+\beta J(A,s))ds}\left[\int_t^1\frac{\partial}{\partial A}J(A,s)ds\right]dt. \end{aligned}$$

Evaluating at $A=0$ we obtain

$$f'(0) = \alpha\gamma\int_0^1 g(0,t)e^{-\mu t-(1-t)\nu}dt.$$

Taking the second derivative yields

$$\begin{aligned}
f''(A) &= 2\alpha\gamma \int_0^1 \left[\frac{\partial}{\partial A} g(A,t)\right] e^{-\mu t} e^{-\int_t^1 (\nu+\beta J(A,s))ds} dt \\
&\quad - 2\alpha\beta\gamma \int_0^1 g(A,t) e^{-\mu t} e^{-\int_t^1 (\nu+\beta J(A,s))ds} \left[\int_t^1 \frac{\partial}{\partial A} J(A,s) ds\right] dt \\
&\quad - 2\alpha\beta\gamma A \int_0^1 \left[\frac{\partial}{\partial A} g(A,t)\right] e^{-\mu t} e^{-\int_t^1 (\nu+\beta J(A,s))ds} \left[\int_t^1 \frac{\partial}{\partial A} J(A,s) ds\right] dt \\
&\quad + \alpha\gamma A \int_0^1 \left[\frac{\partial^2}{\partial A^2} g(A,t)\right] e^{-\mu t} e^{-\int_t^1 (\nu+\beta J(A,s))ds} dt \\
&\quad + \alpha\beta^2\gamma A \int_0^1 g(A,t) e^{-\mu t} e^{-\int_t^1 (\nu+\beta J(A,s))ds} \left[\int_t^1 \frac{\partial}{\partial A} J(A,s) ds\right]^2 dt \\
&\quad - \alpha\beta\gamma A \int_0^1 g(A,t) e^{-\mu t} e^{-\int_t^1 (\nu+\beta J(A,s))ds} \left[\int_t^1 \frac{\partial^2}{\partial A^2} J(A,s) ds\right] dt.
\end{aligned}$$

Note that in this equation, all the terms except the first two have a factor A. Evaluating at $A = 0$ we obtain

$$\begin{aligned}
f''(0) &= 2\alpha\gamma \int_0^1 \left(\left[\frac{\partial}{\partial A} g(A,t)\right]\Big|_{A=0}\right) e^{-\mu t-(1-t)\nu} dt \\
&\quad - 2\alpha\beta\gamma \int_0^1 g(0,t) e^{-\mu t-(1-t)\nu} \int_t^1 \left(\frac{\partial}{\partial A} J(A,s)\right)\Big|_{A=0} ds dt \\
&= 2\alpha\gamma \int_0^1 \left(\left[\frac{\partial}{\partial A} g(A,t)\right]\Big|_{A=0}\right) e^{-\mu t-(1-t)\nu} dt \\
&\quad - 2\alpha^2\beta\gamma \int_0^1 g(0,t) e^{-\mu t-(1-t)\nu} \int_t^1 e^{-\nu s} \int_0^s g(0,r) e^{-\mu r+\nu r} dr ds dt.
\end{aligned}$$

The last line is achieved by using $\frac{\partial}{\partial A} J(A,t)\Big|_{A=0} = \alpha e^{-\nu t} \int_0^t g(0,\tau) e^{-\mu\tau+\nu\tau} d\tau$. This quantity is found by taking the derivative of the differential equation in model (1) with respect to A, solving for $\frac{\partial}{\partial A} J$, and evaluating at $A = 0$. The conclusion of the lemma follows immediately.

□

6.2 Proof of Proposition 2

Proof The definition of T shows $T[B](A,t) \geq 0$ if $B(A,t) \geq 0$. Since $B_0(A,t) \equiv 0$, $B_n(A,t) \geq 0$ for all n. Observe that

$$B_3(A,t) = T[B_2](A,t) \leq T[B_0](A,t) = B_1(A,t),$$

and thus

$$B_4(A,t) = T[B_3](A,t) \geq T[B_1](A,t) = B_2(A,t).$$

Assume for some $k \geq 1$, $B_{2k+1}(A,t) \leq B_{2k-1}(A,t)$ and $B_{2(k+1)}(A,t) \geq B_{2k}(A,t)$. Then $B_{2k+3}(t) = T[B_{2(k+1)}](A,t) \leq T[B_{2k}](A,t) = B_{2k+1}(A,t)$, and thus $B_{2k+4}(t) = T[B_{2k+3}](A,t) \geq T[B_{2k+1}](A,t) = B_{2(k+1)}(A,t)$. Using induction and the fact $B_n(A,t) = T[B_{n-1}](A,t) \leq T[B_0](A,t) \leq B_1(A,t)$, we have

$$
\begin{aligned}
&B_1(A,t) \geq B_3(A,t) \geq \cdots \geq B_{2k-1}(A,t) \geq B_{2k+1}(A,t) \geq \cdots \geq 0,\\
&B_0(A,t) \leq B_2(A,t) \leq \cdots \leq B_{2k}(A,t) \leq B_{2(k+1)}(A,t) \leq \cdots \leq B_1(A,t).
\end{aligned}
$$

Since both $B_{2n}(A,t)$ and $B_{2n+1}(A,t)$ are monotone and bounded in n, we have that $\lim_{n\to\infty} B_{2n+1}(t) = \bar{B}(A,t)$ and $\lim_{n\to\infty} B_{2n}(A,t) = \underline{B}(A,t)$. By taking $n \to \infty$ in $B_{2n+1}(A,t) = T[B_{2n}](A,t)$ and $B_{2(n+1)}(A,t) = T[B_{2n+1}](A,t)$ and using the dominated convergence theorem, we have

$$
\bar{B}(A,t) = T[\underline{B}](A,t), \quad \underline{B}(A,t) = T[\bar{B}](A,t). \tag{9}
$$

(9) and continuity of $\bar{B}(A,t)$ and $\underline{B}(A,t)$ show that $\bar{B}(A,t)$ and $\underline{B}(A,t)$ are differentiable functions. By directly taking the derivatives on both sides of $\bar{B}(A,t) = T[\underline{B}](A,t)$, we obtain

$$
\bar{B}_t = \alpha\gamma e^{-\mu t} g(A,t) + (-\nu - \frac{\beta}{\gamma} A\underline{B}(A,t)) T[\underline{B}](A,t).
$$

Using $T[\underline{B}](A,t) = \bar{B}(A,t)$, we find

$$
\bar{B}_t = \alpha\gamma e^{-\mu t} g(A,t) - \nu\bar{B} - \frac{\beta}{\gamma} A\bar{B}\underline{B}. \tag{10}
$$

Similarly

$$
\underline{B}_t = \alpha\gamma e^{-\mu t} g(A,t) - \nu\underline{B} - \frac{\beta}{\gamma} A\bar{B}\underline{B}. \tag{11}
$$

Subtracting (11) from (10), we find

$$
(\bar{B} - \underline{B})_t = -\nu(\bar{B} - \underline{B}). \tag{12}
$$

(5) shows $\bar{B}(A,0) = \underline{B}(A,0) = 0$. This and (12) indicate $\bar{B}(A,t) \equiv \underline{B}(A,t)$ so that

$$
\bar{B}(A,t) = T[\bar{B}](A,t).
$$

The uniqueness of solution of (1) implies $\bar{B}(A,t) \equiv \underline{B}(A,t) \equiv B(A,t)$. This completes the proof.

□

6.3 Proof of Theorem 2

Proof The condition (2) implies that $f(A) < A$ for small positive A. Since $f(A)$ is continuous, $f(A)$ has a positive equilibrium if and only if there exists $A > 0$ such that $f(A) > A$. According to Proposition 2, as $n \to \infty$, $B_{2n}(A, 1)$ increases to $B(A, 1)$ and $B_{2n+1}(A, 1)$ decreases to $B(A, 1)$. If there is $A > 0$ and $n_0 \geq 1$ such that $B_{2n_0}(A, 1) > 1$, then $B(A, 1) > 1$ which means $f(A) > A$, so that there is a positive equilibrium. If there is $n_0 \geq 1$ such that for all $A > 0$, $B_{2n_0+1}(A, 1) < 1$, then $B(A, 1) < 1$ for all $A > 0$, so that there is no positive equilibrium. Therefore statements (i)-(ii) hold.

Assume that there is a positive equilibrium. Since $f(A) < A$ for small positive A due to (2), continuity of f shows that there exists a smallest positive equilibrium named A^*. Then $f(A) < A$ for $0 < A < A^*$. This shows that for any A_0 with $0 < A_0 < A^*$ the sequence A_n generated by $A_{n+1} = f(A_n)$ has the property that $A_n \to 0$ as $n \to \infty$, so that A^* is the Allee threshold.

□

References

Abubaker S (2008) Effect of plant density on flowering date, yield and quality attribute of bush beans (phaseolus vulgaris l.) under center pivot irrigation system. American Journal of Agricultural and Biological Sciences 3 (4):666–668

Akhmetzhanov AR, Grognard F, Mailleret L (2011) Optimal life-history strategies in seasonal consumer-resource dynamics. Evolution 65(11):3113–3125

Berec L, Angula E, Courchamp F (2007) Multiple allee effects and population management. Trends Ecol Evol 22:185–191

Bewick S, Cantrell RS, Cosner C, Fagan WF (2016) How resource phenology affects consumer population dynamics. The American Naturalist 187(2):151–166

Calabrese JM, Fagan WF (2004) Lost in time, lonely, and single: reproductive asynchrony and the allee effect. American Naturalist 164:25–37

Calabrese JM, Ries L, Matter S, Auckland J, Roland J, Debinski D, Fagan W (2008) Reproductive asynchrony in natural butterfly populations and its consequences for female matelessness. Journal of Animal Ecology 77:746–756

Callahan HS, Pigliucci M (2002) Shade-induced plasticity and its ecological significance in wild populations of arabidopsis thaliana. Ecology 83:1965–1980

Cao Y, Xiao Y, Huang H, Xu J, Hu W, Wang N (2016) Simulated warming shifts the flowering phenology and sexual reproduction of *Cardamine hirsuta* under different planting densities. Scientific Reports 6:27835

CaraDonna PJ, Iler AM, Inouye DW (2014) Shifts in flowering phenology reshape a subalpine plant community. Procedings of the National Academy of Sciences 111(13):4916–4921

Chmura HE, Kharouba HM, Ashander J, Ehlman SM, Rivest EB, Yang LH (2019) The mechanisms of phenology: the patterns and processes of phenological shifts. Ecological Monographs 89:e01337

Clutton-Brock TH, Mcilrath GM, Maccoll ADC, Kansky R, Chadwick P, Manser M, Skinner JD, Brotherton PNM (1999) Predation, group size and mortality in a cooperative mongoose, Suricata suricatta. Journal of Animal Ecology 68:672–683

Connell JH (1971) On the role of natural enemies in preventing competitive exclusion in some marine animals and in rain forest trees. Dynamics of populations, 298(312)

Courchamp F, Berec L, Gascoigne J (2008) Allee effects in ecology and conservation. Oxford University Press, New York

Davis HG, Taylor CM, Lambrinos JG, Strong DR (2004) Pollen limitation causes an allee effect in a wind-pollinated invasive grass (Spartina alterniflora). Proc Natl Acad Sci USA 101:13804–13807

Donohue K (2009) Completing the cycle: maternal effects as the missing link in plant life histories. Philosophical Transactions of the Royal Society B: Biological Sciences 364(1520):1059–1074

Donohue K, Messiqua D, Pyle EH, Heschel MS, Schmitt J (2000) Evidence of adaptive divergence in plasticity: density- and site-dependent selection on shade-avoidance responses in impatiens capensis. Evolution 54:1956–1968

Encinas-Viso F, Revilla TA, Etienne RS (2012) Phenology drives mutualistic network structure and diversity. Ecology Letters 15(3):198–208

Eskola H, Geritz S (2007) On the mechanistic derivation of various discrete-time population models. Bull Math Biol 69:329–346

Eskola H, Parvinen K (2010) The allee effect in mechanistic models based on inter-individual interaction processes. Bull Math Biol 72:184–207

Eskola HT (2009) On the evolution of the timing of reproduction. Theoretical Population Biology 75(2-3):98–108

Fagan W, Bewick S, Cantrell S, Cosner C, Varassin I, Inouye D (2014) Phenologically explicit models for studying plant–pollinator interactions under climate change. Theoretical Ecology 7:289–297

Fagan WF, Cosner C, Larsen EA, Calabrese JM (2010) Reproductive asynchrony in spatial population models: how mating behavior can modulate allee effects arising from isolation in both space and time. The American Naturalist 175(3):362–373

Galloway LF (2002) The effect of maternal phenology on offspring characters in the herbaceous plant campanula americana. Journal of Ecology pp 851–858

Galloway LF (2005) Maternal effects provide phenotypic adaptation to local environmental conditions. New phytologist 166(1):93–100

Galloway LF, Burgess KS (2009) Manipulation of flowering time: phenological integration and maternal effects. Ecology 90(8):2139–2148

Gascoigne J, Berec L, Gregory S, Courchamp F (2009) Dangerously few liaisons: a review of mate-finding allee effects. Population Ecology 51:355–372

Gray DR (2004) The gypsy moth life stage model: landscape-wide estimates of gypsy moth establishment using a multi-generational phenology model. Ecological Modelling 176:155–171

Hale JK (1980) Ordinary Differential Equations. Krieger Publishing Co.

Janzen DH (1970) Herbivores and the number of tree species in tropical forests. The American Naturalist 104(940):501–528

Johnson DM, Liebhold AM, Tobin PC, Bjrnstad ON (2006) Allee effects and pulsed invasion by the gypsy moth. Nature 44:361–363

Keller JA, Shea K (2021) Warming and shifting phenology accelerate an invasive plant life cycle. Ecology 102(1):e03219

Kramer AM, Dennis B, Liebhold AM, Drake JM (2009) The evidence for allee effects. Population Ecology 51:341–354

Lewis MA, Li B (2012) Spreading speed, traveling waves, and minimal domain size in impulsive reaction-diffusion models. Bull Math Biol 74:2383–2402

Logan JA, Powell JA (2001) Ghost forests, global warming, and the mountain pine beetle (Coleoptera: Scolytidae). American Entomologist 47:160

Lynch HJ, Rhainds M, Calabrese JM, Cantrell S, Cosner C, Fagan WF (2014) How climate extremes—not means—define a species' geographic range boundary via a demographic tipping point. Ecological Monographs 84:134–149

Mailleret L, Lemesle V (2009) A note on semi-discrete modelling in the life sciences. Philosophical Transactions of the Royal Society A-mathematical and Engineering 1908:4779–4799

Miller-Rushing AJ, Hoye TT, Inouye DW, Post E (2010) The effects of phenological mismatches on demography. Philosophical Transactions of the Royal Society B: Biological Sciences 365(1555):3177–3186

Mooring MS, Fitzpatrick TA, Nishihira TT, Reisig DD (2004) Vigilance, predation risk, and the allee effect in desert bighorn sheep. Journal of Wildlife Management 68:519–532

Nicholson AJ (1954) An outline of the dynamics of animal populations. Australian journal of Zoology 2(1):9–65

Otto G, Bewick S, Li B, Fagan WF (2018) How phenological variation affects species spreading speeds. Bull Math Biol 80:1476–1513

Pervenecki TJ (2019) Allee effects introduced by density dependent phenology. University of Louisville PhD Thesis

Rhainds M, Fagan WF (2010) Broad-scale latitudinal variation in female reproductive success contributes to the maintenance of a geographic range boundary in bagworms (lepidoptera: Psychidae). PLOS One 5:e14166

Rinella DJ, Wipfli MS, Stricker CA, Heintz RA, Rinella MJ (2012) Pacific salmon (oncorhynchus spp.) runs and consumer fitness: growth and energy storage in stream-dwelling salmonids increase with salmon spawner density. Canadian Journal of Fisheries and Aquatic Sciences 69:73–84

Roach DA, Wulff RD (1987) Maternal effects in plants. Annual review of ecology and systematics 18(1):209–235

Robinet C, Liebhold A, Gray D (2007) Variation in developmental time affects mating success and allee effects. Oikos 116:1227–1237

Robinet C, Lance DR, Thorpe KW, Onufrieva KS, Tobin PC, Liebhold AM (2008) Dispersion in time and space affect mating success and allee effects in invading gypsy moth populations. The Journal of Animal Ecology 77:966–973

Schmitt J, Eccleston J, Ehrahardt D (1987) Density-dependent flowering phenology, outcrossing, and reproduction in impatiens capenis. Oecologia 72:341–347

Thieme HRT (2003) Mathematics in Population Biology. Princeton University Press, Princeton, NJ

Thomas SC, Bazzaz FA (1993) The genetic component in plant size hierarchies: norms of reaction to density in a polygonum species. Ecological Monographs 63:232–249

Tobin PC, Whitmire SL, Johnson DM, Bjørnstad ON, Liebhold AM (2007) Invasion speed is affected by geographical variation in the strength of allee effects. Ecology Letters 10:36–43

Turchin P (1990) Rarity of density dependence or population regulation with lags? Nature 344(6267):660–663

Van Asch M, Julkunen-Tiito R, Visser ME (2010) Maternal effects in an insect herbivore as a mechanism to adapt to host plant phenology. Functional Ecology 24(5):1103–1109

Vermeulen PJ (2015) On selection for flowering time plasticity in response to density. New Phytologist 205(1):429–439

Vincent TL, Brown JS (1984) Stability in an evolutionary game. Theoretical Population Biology 26:408–427

Walter JA, Meixler MS, Mueller T, Fagan WF, Tobin PC, Haynes KJ (2015) How topography induces reproductive asynchrony and alters gypsy moth invasion dynamics. Journal of Animal Ecology 84:188–198

Ward NL, Masters GJ (2007) Linking climate change and species invasion: an illustration using insect herbivores. Global Change Biology 13:1605–1615

Weinig C, Johnston J, German ZM, Demink LM (2006) Local and global costs of adaptive plasticity to density in arabidopsis thaliana. American Naturalist 167:826–836